Journal of Luminescence 202 (2018) 322–326

Contents lists available at ScienceDirect

Journal of Luminescence

journal homepage: www.elsevier.com/locate/jlumin

Selective dependence of the electron-phonon interaction on the nature of the optical transition in AlGaAs quantum wells

Cássio Sanguini Sergio[a], Celso de Araujo Duarte[b,*], Carlos Eduardo Arévalo Anzola[c], Gilmar Macêdo de Aquino[c], Guennady Michailovich Gusev[d]

[a] Departamento de Física, Universidade Federal de Roraima, Av. Cap. Ene Garcez, 2413, 69310-000 Boa Vista (RR), Roraima (RR), Brazil
[b] Departamento de Física, Universidade Federal do Paraná, CP 19044, 81531-990 Curitiba (PR), Brazil
[c] Programa de Pós Graduação em Física, Universidade Federal de Roraima, Roraima (RR), Brazil
[d] Depto. de Física dos Materiais e Mecânica, Instituto de Física, Universidade de São Paulo, 05508-090 São Paulo (SP), Brazil

ARTICLE INFO

Keywords:
Electron-phonon interaction
AlGaAs
Quantum well
Photoluminescence

ABSTRACT

In the present work, it is carried out a study of the optical emission of $Al_xGa_{1-x}As/GaAs$ quantum wells by photoluminescence (PL). A detailed analysis of the thermal redshift of the (PL) peaks showed that strength of the electron-phonon interaction is influenced by the degree of binding of the electron in the conduction band (free or localized excitonic state, bulk or quantum size confined state).

1. Introduction

One of the main characteristics of the semiconductors is the band gap energy E_g that separates the conduction and the valence bands, being the conduction band (CB) empty and the valence band (VB) full at zero kelvin temperature. The band gap energy can be determined by optical measurements, e.g. through photoluminescence (PL). In PL measurements, the sample is pumped with a laser beam, and the energy of the incident photon $h\nu$ (where ν is the frequency of the light of the laser beam) is absorbed by an electron of the VB. If $h\nu \geq E_g$, this electron is promoted to the CB, and suffers a series of non radiative processes until it reaches the bottom of the CB. Once in the bottom of the CB, it returns to the VB emitting a photon with exactly the energy $\varepsilon = E_g$. Determining the frequency ν_{em} of the emitted photon is enough to get the band gap energy by the formula $E_g = h\nu_{em}$.

It is a well-known matter of fact the dependency of the band gap energy E_g with respect to the temperature [1,2]. The band gap energy is a monotonic decreasing function of the temperature, and this redshift is known as *gap shrinkage*. The gap shrinkage is today attributed to the electron-phonon interaction combined with non vanishing contributions of the thermal expansion mechanism [3]. Based on the relevance of the electron-phonon interaction on the gap shrinkage, Viña et al. [4] and Pässler [5] proposed theoretically based formulas. In particular, the formula proposed by Pässler is given by:

$$E_g(T) = E_{g0} - \frac{\alpha \cdot \Theta}{2} \cdot \left[\sqrt[p]{1 + \left(\frac{2\,T}{\Theta}\right)^p} - 1 \right], \tag{1}$$

where $\Theta \equiv \hbar\omega/k$, and $\hbar\omega$ is the effective phonon energy. Parameters α and Θ have a theoretical basis associated to the electron-phonon interactions, being the parameter p empirically adjusted. Expression (1) is one of the most cited expressions for the temperature variation of the energy gap, and studies show that it provides the best adjusts to the experimental results [6–9].

While the parameters α and Θ have physical meaning, parameter p apparently introduces the arbitrariness of an empirical Ansatz, breaking the rigor of the strictly theoretical basis of Pässler formula (1). However, Pässler showed that p is directly associated to the electron-phonon spectral function [10] and usually $p \approx 2.7$ [3].

The present work is dedicated to the application of Pässler formula (1) to experimental values of $E_g(T)$ obtained from PL measurements in epitaxially grown $Al_xGa_{1-x}As$ quantum wells (QW). Focusing on the value of the exponent p, we show that the strength of the electron-phonon interaction depends on the nature of the optical transition.

2. Description of the samples and the experimental technique

Three square 140 Å-wide $Al_xGa_{1-x}As$ QW's were grown by molecular beam epitaxy (MBE) in GaAs [100] substrates. The three samples were remotely doped with two Si-delta layers placed 250 Å far from the QW's, which were placed between superlattice AlGaAs barriers with an

* Corresponding author.
E-mail address: celso@fisica.ufpr.br (C.d.A. Duarte).

https://doi.org/10.1016/j.jlumin.2018.05.072
Received 4 December 2017; Received in revised form 2 May 2018; Accepted 29 May 2018
Available online 31 May 2018

effective Al content of 31%. The samples differed by the Al content inside the quantum well, as follows: sample QW 3224: 0.0%; sample QW 3249: 9.4%; and sample QW 3236: 13%. The detailed description of the architecture of the samples is presented here: (1) a 1 μm wide GaAs buffer was grown directly over the substrate; (2) after that, a 500 Å-wide linear gradient ramp from x = 0 up to x = 30%; (3) then, a 1000 Å-wide digital AlAs/GaAs superlattice (effective stoichiometric Al fraction: 30%); (4) a Si-delta doping layer (areal density: 2.3×10^{12} cm^{-2}); (5) a digital AlAs/GaAs superlattice spacer layer (width: 250 Å; effective Al content: 30%); (6) the grown of the QW with the desired Al content; (7) a second identical spacer layer; (8) a second identical Si-delta doping layer; (9) a 400 Å wide digital AlGaAs layer (effective stoichiometry: x = 30%); (10) a third Si-delta doping layer; (11) a 200 Å-wide AlGaAs layer; and (12) a 100 Å-wide GaAs cap layer. The first two Si-delta layers provided the doping of the QW, while the third served to neutralize the charge of dangling bonds in the surface of the samples. Low temperature (~ 1.6 K) Hall effect and Shubnikov-de Haas measurements provided the following electron sheet densities in the QW's: sample QW 3224, 9.6×10^{11} cm^{-2}; sample QW 3249, 5.5×10^{11} cm^{-2}; and sample QW 3236, 3.34×10^{11} cm^{-2}.

PL measurements were carried out with a diode-pumped solid-state (DPSS) laser with the wavelength 532 nm and 100 mW power. The spectral analysis was carried with an Andor Shamrock SR-500 monochromator with focal length 500 mm and f/6.5 aperture, with slit aperture 10 μm, coupled to a Andor iDus CCD series 401 and 26×26 μm^2 pixels. The samples were placed on a Janis CCS-100/204N cryostat cooled by a closed cycle He refrigerator, covering the range of temperatures from 10 K up to 300 K.

3. Results and discussion

Fig. 1 presents a cascade of temperature PL spectra for QW 3224 (x = 0%). The inspection of the bare temperature cascade spectra of Fig. 1 (without any mathematical fitting procedure) reveals three peaks: in the main Fig. 1a, a peak centered on about 1.544 and another on about 1.545 eV, and in the Fig. 1b, a very small peak at about 1.555 eV. The eligible optical transitions involve the electron-heavy hole (e-hh) and the electron-light hole (e-lh) pairs, whose confined ground states in quantum well structures are in this order of increasing energy. The energy of these transitions may be reduced in a few meV with the formation of the hydrogen-like electron-hole bound state, the free exciton (FX). Fluctuations of the potential may account for tiny (very few meV) variations of the exciton (X) energy, resulting the localized exciton (LX). Other typical optical transitions involve the binding to an intrinsic acceptor state (A) or a donor state (D) of the semiconductor [11], which reduces the energy by an amount that varies in a wide range from about a dozen to hundreds of meV, and are discarded, since we deal with in high purity MBE-grown epilayers. Owing to the high electron doping in our samples we eventually see the formation of the negatively charged exciton, the trion (X^-), with an energy very close below that of the X [12–15].

The peak-to-peak energy difference in Fig. 1a is of the order of ~ 1.5 meV, suggesting that the high energy peak corresponds to a FX (e,hh) transition, and that the low energy peak corresponds to a X^-, or LX, or both transitions. The peak at 1.555 eV in Fig. 1b is about ~ 10 meV above the e-hh FX, and by this reason we attribute it to a FX (e,lh) transition.

In face of this, we expect the following hierarchy of peaks, by increasing the energy: 1) the e-hh states at/or around ~ 1.544 eV, corresponding to either the X^- or the LX state, or both merged (see the main Fig. 1a), and at 1.545 eV (an FX state, same Figure); and 2) an e-lh FX state, see Fig. 1b. The X^- and the LX peaks cannot be distinguished in with our experimental data, nevertheless being irrelevant for the purpose of the present work. In any way, for the case of the existence of only one of them (either the X^- or the LX state), we made a two-Lorentzian fit to resolve this peak from the hh FX state, obtaining the following activation energies from the integrated intensity Arrhenius plot: 0.9 meV (LX/X^-) and − 3 meV (FX hh). These activation energies do not show a direct relation with the average 1.5 meV peak separation. In face of this, we proceeded the three-Lorentzian fit (a typical fitting is shown in the top-right inset for the 24 K spectrum on Fig. 1a) and an Arrhenius plot of the integrated intensities (see the top-right inset of Fig. 3a) resulted the activation energy of 0.6 meV for the lowest energy peak, 0.1 meV for the middle energy peak, and − 1.5 meV for the

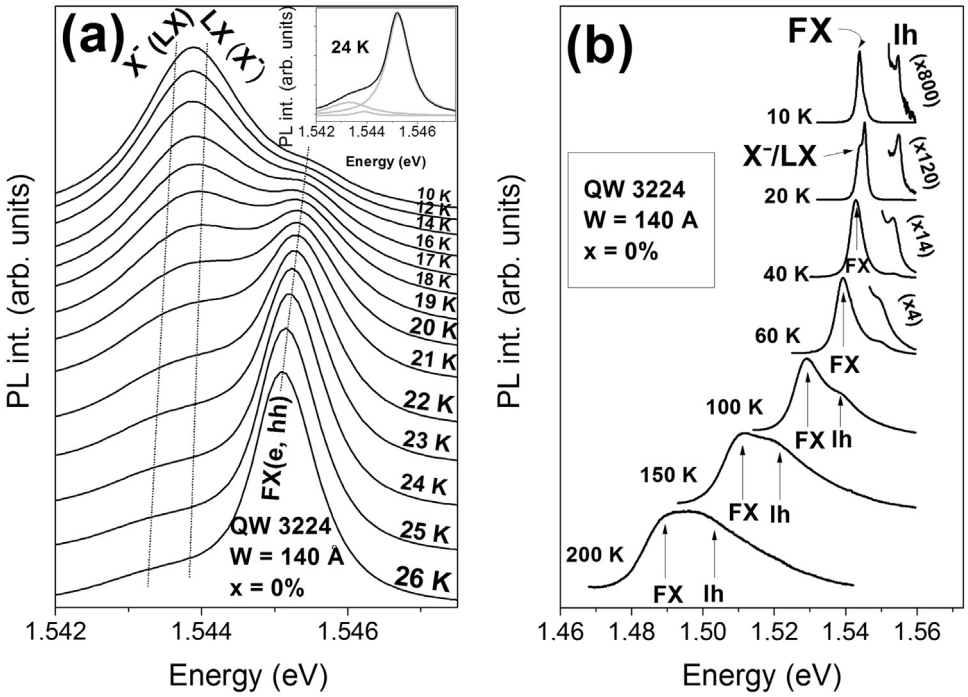

Fig. 1. PL spectra of QW 3224 (x = 0%) at various temperatures, where we identified: (a) the X^- (or LX(e, hh)) and the LX(e, hh) (or X^-) peaks, and the FX(e, hh) peak; and (b) the lh X(e-lh) peak. The top-right inset in (a) shows the three fitted Lorentzians (gray) for the spectrum at 24 K (black).

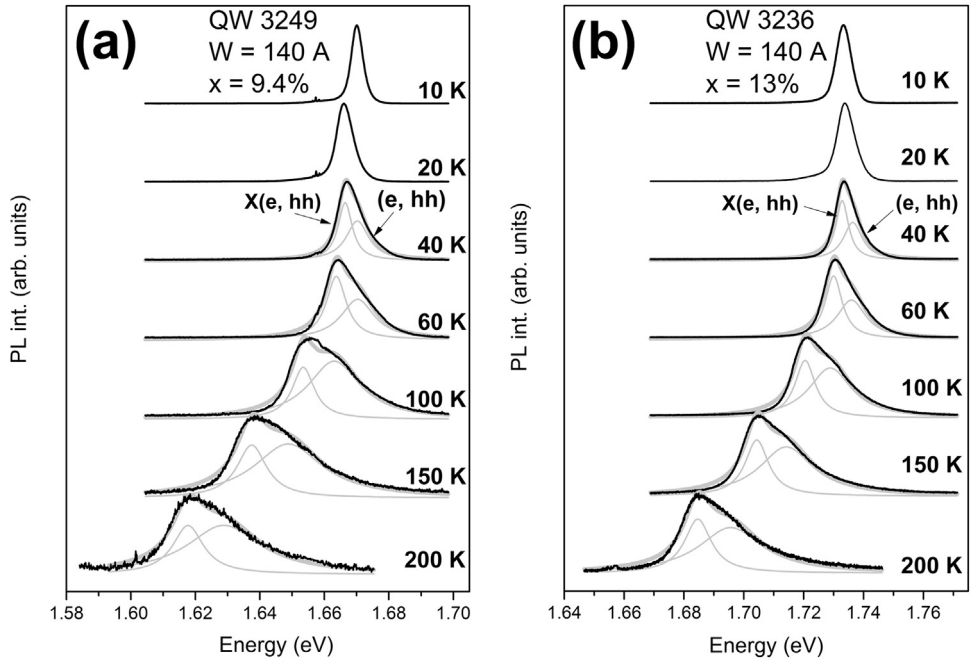

Fig. 2. PL spectra of QWs (a) 3249 ($x = 9.4\%$) and (b) 3236 ($x = 13\%$) vs. temperature, showing X(e, hh) and (e, hh) peaks. The gray lines are two fitted Lorentzian curves.

highest energy peak. The 0.6 meV is similar to the average energy separation between the lowest and the middle energy peaks, and the 1.5 meV is similar to the average energy separation between the middle and the highest energy peaks (see the bottom-left inset of Fig. 3a). This is in accordance with a thermal activation mechanism from the lowest energy to the middle energy peak, and from the middle energy to the higher energy peak, suggesting the coexistence of LX and X^- states. Note that both the LX and X^- states exist up to 26 K (see Fig. 1a), disappearing at higher temperatures due to the thermal activation.

Fig. 2 shows the temperature dependent PL spectra for QWs (a) 3249 ($x = 9.4\%$) and (b) QW 3236 ($x = 13\%$), characterized by single wide peaks at low temperatures that split above ~ 40 K, being resolved by two-Lorentzian curve fit. The peak assignments in the AlGaAs layers are analogous to the GaAs case [16]. We attribute the resolved peaks to an excitonic transition X(e,hh) (lowest energy peak) and a subband-to-subband transition (e,hh). The separation in energy between these two peaks is characteristic of an exciton binding energy, and by this reason we do not attribute the highest energy one to a lh state transition. Yet, the wide peak broadening prevent to resolve FX, LX or even X^- states.

Once identified all the optical transitions, we proceed to a study of the temperature variation of peak positions. Fig. 3 shows the plots of the temperature dependence of the energies at the peak centers (main figures). The bottom-left insert in Fig. 1(a) shows the low temperature positions of the X^-, LX and FX peaks (X^- and LX quench above ~ 26 K, and are not shown in the main Fig. 3(a)).

The top-right inserts of Figs. 3(b) and (c) show the energy differences between the X(e-hh) and (e,hh) peak centers that physically correspond to the exciton binding energies Δ_X. From the literature we extract the approximate value $\Delta_X = 4 - 5$ meV [17], which is almost equal to the zero temperature value in both insets (~ 4 meV). However, a temperature dependence of Δ_X is not expected, and consequently the energy differences in both insets must contain an additional term contribution. We ascribe this to the yet reported effect of quantum well barrier composition fluctuation, that results in a blue shift of the peak center position at low temperatures [18]. This is consistent with the fact that the effect occurred only on the two nonzero-Al-content samples, where composition fluctuation is expected and being absent on sample 3224 (0% Al).

The center positions of the main peaks (that persisted up to high temperatures) were fitted with Pässler's formula (Eq. (1)) on the range of temperatures 10 – 300 K, showing an excellent fit.

Table 1 shows the values of the fitted parameters for the three samples. In the fitting, it was employed the temperature $\Theta = 222.4$ K [5], which is related to the Debye temperature Θ_D by $\Theta \approx (2/3)\Theta_D$. The values of the fitted parameter α lie on the range 0.44–0.49 meV/K, and are consistent with the literature ($\alpha = 0.475$ meV/K for pure GaAs [3]). On the other side, the exponent parameter p differs selectively according to the nature of the optical transition: for excitons, p lies on the narrow range 2.0–2.3; for (e,hh) transitions, p lies on 3.4–3.5; and finally, for pure the GaAs band-to-band transition, $p = 2.5$. The dependency of p with respect to the nature of the optical transition leads to consider the issue in detail. Following Pässler [10], $p = \mu + 1$, where μ is the exponent in Pässler Ansatz of a nonlinear power-law type electron-phonon spectral function $f(\varepsilon)$

$$f(\varepsilon) = \begin{cases} (\mu\alpha/k)(\varepsilon/\varepsilon_0)^{\mu} & (\varepsilon \le \varepsilon_0), \\ 0 & (\varepsilon > \varepsilon_0), \end{cases} \tag{2}$$

being $\varepsilon_0 = (\mu + 1)/\mu \cdot k\Theta$ a cutoff energy, and

$$E_g(T) = E_{g0} - \int d\varepsilon f(\varepsilon)\left(\overline{n}(\varepsilon, T) + \frac{1}{2}\right), \tag{3}$$

where $\overline{n}(\varepsilon, T) = (coth(\varepsilon/(2kT) - 1)$ is the thermally averaged occupation number of phonons. Table 1 also lists the values of μ and the character of the spectral function, revealing that excitonic transitions are slightly nonlinear ($1 < \mu < 1.3$) while subband-to-subband transition in QW is supralinear between quadratic and cubic ($\mu \approx 2.5$), and bulk GaAs band-to-band transition is supralinear in the intermediate regime between linear and quadratic ($\mu \approx 1.5$).

Fig. 4 shows the plot of Eq. (2) in dimensionless form $f(\varepsilon) \times (\alpha/k)^{-1}$ as a function of ε, revealing that the increase of μ results in the quenching of the low energy phonon contribution, accompanied by the rise up of the higher energy phonon one. Also, for larger μ, the area below the curve of $f(\varepsilon)$ increases (algebric integration shows that the integral of $f(\varepsilon)$ varies as μ^2). This leaves to the misleading conclusion that for large μ the gap shrinkage (Eq. (3)) is larger. As we will see, the exponential character of Bose-Einstein statistics in $\overline{n}(\varepsilon, T)$ is dominant,

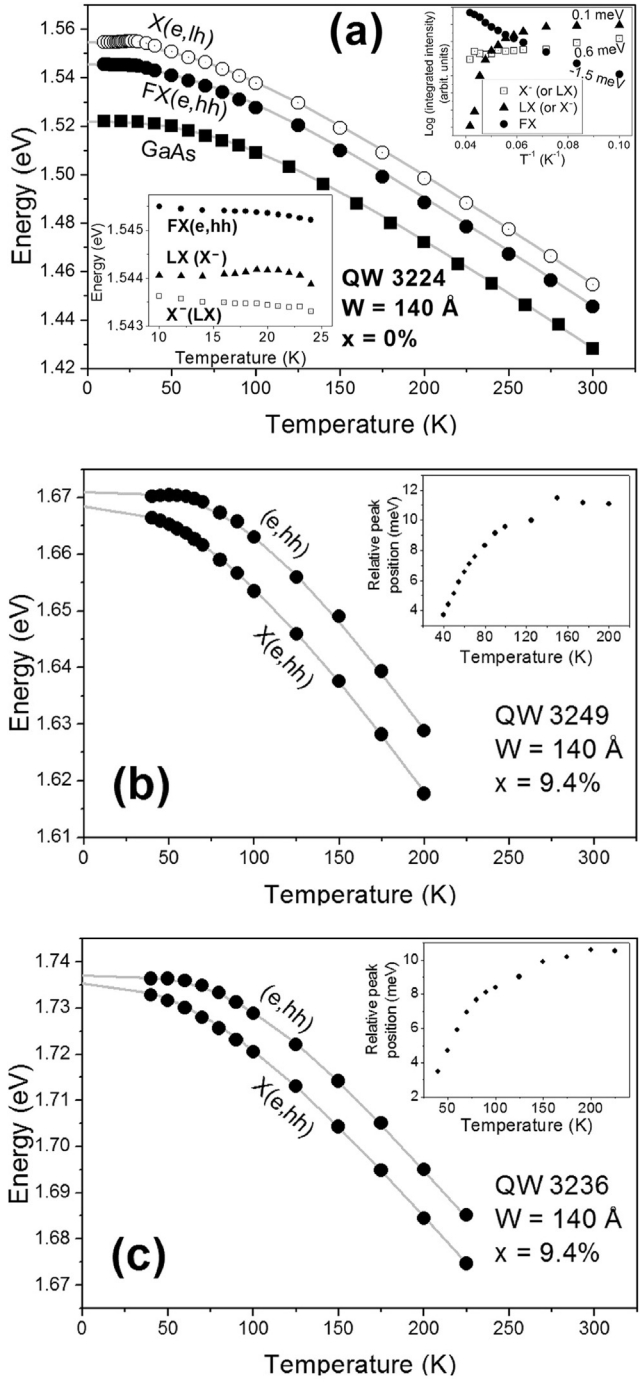

Fig. 3. Evolution of the transition energies, extracted from the corresponding peak positions in Figs. 1 and 2, as a function of temperature. The experimental data (geometrical symbols) were fitted using the equation of Pässler (1) (gray continuous lines). The bottom-left insert in Fig. (a) shows the X^- (or LX), the LX (or X^-) and the FX peak positions at low temperatures, and the top-right insert shows their corresponding Arrhenius plots. The top right insertions in Figs. (b, c) present the X(e, hh) binding energies as a function of the temperature.

leaving exactly to the opposite result. After some algebra, the integral in Eq. (3) reduces to

$$I(\mu, \tau) = \tau^{\mu+1}(\mu + 1) \int_0^{1/\tau} dx x^{\mu} [cothx - 1] \quad (4)$$

(in units of $\alpha\Theta$) where $\tau = 2\mu/(\mu + 1)T/\Theta$ is the normalized temperature.

Fig. 5 shows the log-scale plot of $I(\mu, \tau)$ as a function of μ for some values of τ (in our experimental conditions $\tau < 3$). The plot reveals that the gap shrinkage (Eq. (3)) is expected to be larger for smaller values of μ, when the electron-phonon interaction is larger, and consequently that the excitonic states in our samples (smallest values of μ) are the most affected by the electron-phonon coupling, while the quantum size confined state of the QW is less affected (highest values of μ). To explain this, note that the exciton is the electron-hole binding. Ultimately

Table 1
The list of the fitted parameters p and α of the Pässler formula for all the samples, being the parameter $\Theta = 222.4$ K kept fixed. It was not possible to fit the Pässler formula for the LX(e,hh) (sample QW 3224) due to the scarce experimental data. The standard deviation of the fitted parameters α and p lay on the 3rd significant digit, and that of E_{g0} on the 4th. The last two columns present the values of the exponent μ and the character of the spectral function $f(\varepsilon)$ (see Eq. (2)).

QW	x (%)	State	p	α (meV/K)	E_{g0} (eV)	μ	Kind
3224	0.0	LX(e,hh)	–	–	–	–	–
		FX(e,hh)	2.03	0.487	1.5462	1.03	Linear
		X(e,lh)	2.06	0.488	1.5557	1.06	
3249	9.4	X(e,hh)	2.26	0.458	1.6689	1.26	
		(e,hh)	3.55	0.445	1.6712	2.55	
3236	13.0	X(e,hh)	2.35	0.458	1.7348	1.35	Supralin.
		(e,hh)	3.40	0.436	1.7373	2.40	
bulk	0.0	(e,hh)	2.51	0.474	1.5224	1.51	

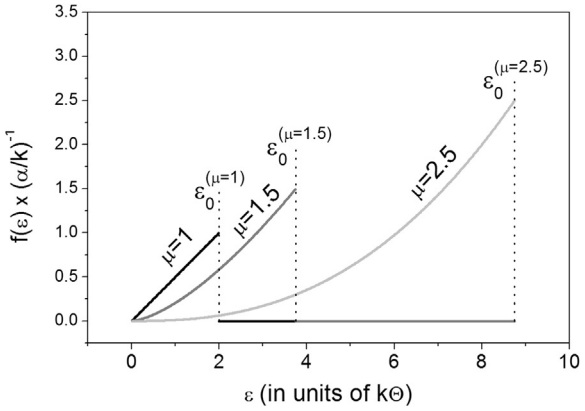

Fig. 4. Plot of $f(\varepsilon) \times (\alpha/k)^{-1}$ as a function of ε (in units of $k\Theta$) for three representative values of μ (similar to the values presented on Table 1). The corresponding values of the cutoff energy $\varepsilon_0^{(\mu)}$ are marked by vertical dotted lines. Note that as μ increases, the contribution from low energy phonons (low values of ε) gives place to higher energy phonons.

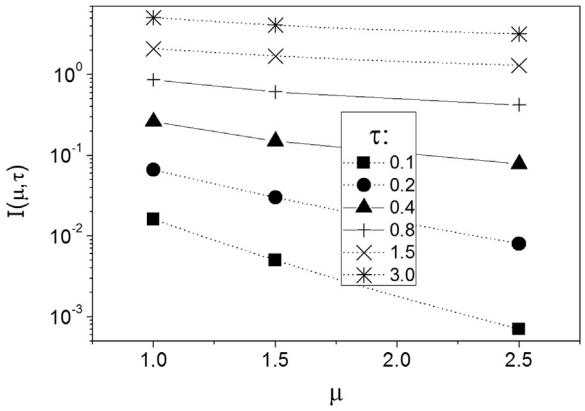

Fig. 5. The plot of $I(\mu, \tau)$ as a function of μ (three representative values) and different values of the normalized temperature τ. The lines are guides to the eyes.

the hole is a single positive, unpaired elementary charge + e in the nucleus of an atom. Since the all the atoms are in vibration in the lattice, the excitonic states are directly influenced by the interaction with phonons. On the other side, in simple unbound band-to-band states (e,hh), (e,lh) the electrons are not strongly bound to holes and the phonon influence should be lower. The bulk GaAs (e,hh) transition, for which μ lies on the intermediate values between the excitonic and the quantum size confined states, is thus less affected than the excitonic states. By the other side, the bulk state is more affected than the quantum size confined state. We are led to the conclusion that possibly the quantum size confinement "freezes" the photo generated electron and hole states in the QW's, preventing their interaction with the vibrating atoms of the lattice.

Finally, note that Θ_D depends on the Al content [19]. In our samples, x= 0.0–13.0% so $\Theta \approx (2/3)\Theta_D \approx 224 - 225$K, resulting in negligible changes in ε_0, keeping the integral in Eq. (3) unchanged. We conclude that the increase in Θ_D does not account for the observed changes of μ. Note also that the exciton Bohr radius in AlGaAs is 90 Å, which is smaller than the size of our QW's. Consequently, quantum size confinement does not affect the excitons (does not "freeze" the exciton).

4. Conclusions

We verified an excellent fit of the experimental data to Pässler formula, Eq. (1). The interaction of photo generated carriers with the lattice phonon showed to depend selectively on the nature of the electron-hole state (excitonic, quantum size confined, unbound bulk).

Acknowledgements

The authors thank the LMBE of Prof. Dr. A.A. Quivy (Inst. of Physics, USP) for the QW samples.

References

[1] H. Fesefeldt, Der Einfluss der Temperatur auf die Absorptionsspektra der Alkalihalogenidkristalle, Z. Phys. 64 (1930) 623.
[2] Y.P. Varshni, Temperature dependence of the energy gap in semiconductors, Physica 34 (1967) 194.
[3] R. Pässler, G. Oelgart, Appropriate analytical description of the temperature dependence of exciton peak positions in GaAs/$Al_xGa_{1-x}As$ multiple quantum wells and the $\Gamma_{8v} - \Gamma_{6c}$ gap of GaAs, J. Appl. Phys. 82 (1997) 2611–2616.
[4] L. Viña, S. Logothetidis, M. Cardona, Phys. Rev. B 30 (1984) 1979.
[5] R. Pässler, Comparison of different analytical descriptions of the temperature-dependence of the indirect energy gap in silicon, Solid-State Electr. 39 (1996) 1319–1996.
[6] S.A. Lourenço, I.F.L. Dias, J.L. Duarte, E. Laureto, E.A. Meneses, J.R. Leite, I. Mazzaro, J. Appl. Phys. 89 (2001) 6159.
[7] A. Caballero-Rosas, C. Mejía-García, G. Contreras-Puentea, M. López-López, Thin Solid Films 490 (2005) 161.
[8] J.S. Rojas-Ramírez, R. Goldhahn, P. Moser, J. Huerta-Ruelas, J. Hernández-Rosas, M. López-López, J. Appl. Phys. 104 (2008) 124304.
[9] C. Mejía-García, A. Caballero-Rosas, M. López-López, A. Winter, H. Pascher, J.L. López-López, Thin Solid Films 518 (2010) 1825.
[10] R. Pässler, Basic model relations for temperature dependencies of fundamental energy gaps in semiconductors, Phys. Status Sol. (b) 200 (1997) 155–172.
[11] J.I. Pankove, Optical Processes in Semiconductors, 2nd ed., Dover, 2010.
[12] K. Kheng, R.T. Cox, Y. Merle d'Aubigne, Franck Bassani, K. Saminadayar, S. Tatarenko, Observation of negatively charged excitons X^- in semiconductor quantum wells, Phys. Rev. Lett. 71 (1993) 1752.
[13] A.J. Shields, M. Pepper, M.Y. Simmons, D.A. Ritchie, Spin-triplet negatively charged excitons in GaAs quantum wells, Phys. Rev. B 52 (1995) 7841.
[14] V.V. Solovyev, I.V. Kukushkin, Measurement of binding energy of negatively charged excitons in GaAs/$Al_{0.3}Ga_{0.7}As$ quantum wells, Phys. Rev. 79 (2009) 233306.
[15] L. Bryja, J. Jadczak, K. Ryczko, M. Kubisa, J. Misiewicz, A. Wójs, F. Liu, D.R. Yakovlev, M. Bayer, C.A. Nicoll, I. Farrer, D.A. Ritchie, Thermal dissociation of free and acceptor-bound positive trions from magnetophotoluminescence studies of high quality GaAs/AlxGa1-xAs quantum wells, Phys. Rev. B 93 (2016) 165303.
[16] P.J. Pearah, W.T. Masselink, J. Klem, T. Henderson, H. Morkoç, C.W. Litton, D.C. Reynolds, Low-temperature optical absorption in $Al_xGa_{1-x}As$ grown by molecular-beam epitaxy, Phys. Rev. B 32 (1985) 38573861.
[17] L. Pavesi, M. Guzzi, Photoluminescence of $Al_xGa_{1-x}As$ alloys, J. Appl. Phys. 75 (1994) 4779–4842.
[18] S.A. Lourenço, M.A.T. da Silva, I.F.L. Dias, J.L. Duarte, E. Laureto, Correlation between luminescence properties of $Al_xGa_{1-x}As$/GaAs single quantum wells and barrier composition fluctuation, J. Appl. Phys. 101 (2007) 113536.
[19] S. Adachi, GaAs, AlAs, and AlxGa1-xAs: material parameters for use in research and device applications, J. Appl. Phys. 58 (1985) R1–R29.